0026-895X/09/7602-425–439$20.00
MOLECULAR PHARMACOLOGY
Vol. 76, No. 2
57380/3500503
Mol Pharmacol 76:425–439, 2009
Printed in U.S.A.

Estrogen Receptor α, Fos-Related Antigen-2, and c-Jun Coordinately Regulate Human UDP Glucuronosyltransferase 2B15 and 2B17 Expression in Response to 17β-Estradiol in MCF-7 Cells

Dong Gui Hu and Peter I. Mackenzie

Department of Clinical Pharmacology, Flinders University School of Medicine, Flinders Medical Centre, Bedford Park, Australia

Received April 30, 2009; accepted June 1, 2009

ABSTRACT

UDP-glucuronosyltransferase 2B15 and 2B17 expression is upregulated by 17β-estradiol in MCF-7 breast cancer cells, as assessed by quantitative real-time polymerase chain reaction. Using 5′-deletion mapping and site-directed mutagenesis, we demonstrate that 17β-estradiol activation of *UGT2B15* gene transcription is mediated by a 282-base pair fragment positioned −454 to −172 nucleotides from the translation start site. This region contains two putative activator protein-1 (AP-1) elements, one imperfect estrogen response element (ERE), and two consensus ERE half-sites. We propose that these five sites act as an estrogen response unit (ERU), because mutation in any site reduces activation of the *UGT2B15* promoter by 17β-estradiol. Despite the presence of two AP-1 elements, the *UGT2B15* promoter is not responsive to the AP-1 activator phorbol 12-myristate 13-acetate. Although electrophoretic mobility shift assays (EMSA) indicate that the AP-1 proteins c-Jun and Fos-related antigen 2 (Fra-2) bound to the distal AP-1 site, binding of Jun or Fos family members to the proximal AP-1 site was not detected by EMSA. Chromatin immunoprecipitation assays showed a 17β-estradiol-induced recruitment of estrogen receptor (ER) α, c-Jun, and Fra-2 to the 282-bp ERU. The involvement of these three transcription factors in the stimulation of *UGT2B15* gene expression by 17β-estradiol was confirmed by siRNA silencing experiments. Mutagenesis and siRNA experiments indicate that *UGT2B17* expression is also regulated by 17β-estradiol via the ERU, which is fully conserved in both promoters. Because UGT2B15 and UGT2B17 inactivate steroid hormones by glucuronidation, the regulation of their genes by 17β-estradiol may maintain steroid hormone homeostasis and prevent excessive estrogen signaling activity.

Estrogen signaling is mediated by estrogen receptors (ERα and ERβ) via genomic and nongenomic pathways (Marino et al., 2006). In the classic genomic pathway, ER binds as a dimer to an estrogen response element (ERE) in the regulatory regions of target genes to control gene transcription. The ideal or consensus ERE is a 13-bp sequence (5′-GGTCAnnnTGACC-3′; n, any nucleotide), which was first discovered in the 5′-flanking region of the *Xenopus laevis vitellogenin A2* gene (Klein-Hitpass et al., 1986). However, genomic regions termed estrogen response units (ERU) are also capable of enhancing transcription in the presence of estrogen. These ERUs may extend over several hundred nucleotides and contain many imperfect EREs (these deviate by 1–3 bp from the consensus) and ERE half-sites, which act synergistically to achieve high estrogen inducibility (Klein-Hitpass et al., 1988; Klinge, 2001). Indeed, mapping of human ER binding sites in the MCF-7 genome showed that 25% of the identified in vivo ERα binding sites bore only half-EREs or imperfect EREs (Klinge, 2001; Lin et al., 2007). ER can also regulate gene transcription by modulating the activities of other transcriptional factors, such as activator protein-1 (AP-1), nuclear factor-κB and stimulating protein-1 (Kushner et al., 2000; Marino et al., 2006; Safe and Kim, 2008). In this nonclassic pathway, ER does not bind DNA; rather, it interacts with

The work was supported by the National Health and Medical Research Council (NHMRC) of Australia. P.I.M. is a Senior Principal Research Fellow of the NHMRC.

Article, publication date, and citation information can be found at http://molpharm.aspetjournals.org.

doi:10.1124/mol.109.057380.

ABBREVIATIONS: ER, estrogen receptor; ERE, estrogen response element; bp, base pair(s); ERU, estrogen response unit; AP-1, activator protein-1; AR, androgen receptor; FBS, fetal bovine serum; DCC, dextran-coated charcoal; RT, reverse transcription; PCR, polymerase chain reaction; PBS, phosphate-buffered saline; EMSA, electrophoretic mobility shift assay; BSA, bovine serum albumin; PMA, phorbol 12-myristate 13-acetate; UGT, UDP glucuronosyltransferase; WT, wild type; GAPDH,glyceraldehyde-3-phosphate dehydrogenase; fra-2, Fos-related antigen 2; TPA, 12-*O*-tetradecanoylphorbol 13-acetate; TRE, TPA response element; MMP, matrix metalloproteinase; ChIP, chromatin immunoprecipitation; MT, mutant.

bound transcription factors via protein-protein contacts to stabilize DNA-protein complexes and/or recruit coregulators.

Signaling initiated by 17β-estradiol binding to ER is essential for epithelial cell proliferation and ductal development in the breast. Unfortunately, this capacity of 17β-estradiol to stimulate cell proliferation is also a contributor to breast cancer development and progression (Bocchinfuso and Korach, 1997). The factors that control the balance between these beneficial and potentially adverse effects of 17β-estradiol on the breast are poorly understood, but seem to depend on complex interactions between male and female hormones and growth factors.

Androgen signaling through the androgen receptor is an important modifier of estrogen action (Murphy and Watson, 2002). Breast cells contain androgen receptor (AR), and accumulating evidence supports a significant role for androgens as negative modulators of estrogen action in the mammary gland. This evidence includes their capacity to antagonize the effects of estrogens in normal breast development (i.e., to act as anti-estrogens) and their ability to inhibit the basal and estradiol-stimulated growth of AR-positive breast cancer cell lines, including MCF-7 (Andò et al., 2002). Given this antagonistic interaction between androgen and estrogen signaling pathways in breast cells, the differential inactivation and elimination of androgens and estrogens may be an important determinant of the cell or organ's response to these hormones.

The capacity of steroid hormones to bind to their receptors is inhibited by glucuronidation. In addition, steroid glucuronides are more hydrophilic and more readily excreted than steroids. These two outcomes of glucuronidation ensure termination of steroid signaling effects, as aptly illustrated in the prostate (Chouinard et al., 2007). There are 19 functional human UGTs grouped into one family containing nine members (UGT1A1, UGT1A3–UGT1A10) and a second composed of 10 members (UGT2A1–UGT2A3, UGT2B4, UGT2B7, UGT2B10, UGT2B11, UGT2B15, UGT2B17, and UGT2B28) (Mackenzie et al., 2005). However, only a few of these 19 UGTs glucuronidate biologically active steroids to any significant extent. The active androgens testosterone and dihydrotestosterone are exclusively glucuronidated by UGT2B15 and UGT2B17, whereas the biologically active estrogen 17β-estradiol is primarily glucuronidated by UGT1A1, UGT1A3, and UGT1A10 (Chouinard et al., 2006, 2007; Itäaho et al., 2008). The 17β-OH group of the active androgens is the site of glucuronidation, whereas the major metabolite of 17β-estradiol is the 3-OH glucuronide, although recent evidence suggests that UGT2B7 and UGT2B17 are also quite active in forming the 17β-OH glucuronide of this estrogen (Itäaho et al., 2008). Given that UGT2B15 and -2B17 are the only UGTs capable of terminating the effects of active androgens, the mechanisms that control their expression in breast are likely to be of considerable importance in modulating this organ's response to hormones. However, little is known about these mechanisms.

A recent study reported that *UGT2B15* expression in MCF-7 cells is up-regulated by estradiol (Harrington et al., 2006). However, the mechanisms mediating this regulation have not been identified. In the present study, we show that *UGT2B17* in addition to *UGT2B15* is induced by 17β-estradiol in MCF-7 cells and demonstrate that this process is mediated by an ERU containing multiple AP-1 and ERE elements, which are completely conserved in both promoters.

Materials and Methods

Cell Culture, RNA Extraction, and Reverse Transcription. The breast cancer cell line MCF-7, obtained from the American Type Culture Collection (Manassas, VA) was maintained in RPMI 1640 medium (Invitrogen, Carlsbad, CA) supplemented with 5% (v/v) fetal bovine serum (FBS) at 37°C in a 5% CO_2 atmosphere. For 17β-estradiol treatments, MCF-7 cells were cultured for 3 days in phenol red-free RPMI 1640 medium containing 5% dextran-coated charcoal (DCC)-stripped FBS and then plated into six-well plates at a density of 5×10^5 cells/well in 3 ml of fresh medium. After 72 h, cells were treated with either 10 nM 17β-estradiol or 0.1% ethanol (vehicle) for a further 24 h. Total RNA was extracted using the RNeasy Midi Kit (QIAGEN, Valencia, CA) according to the manufacturer's instructions. Reverse transcription (RT) was carried out using reagents from Invitrogen. In brief, total RNA (~1 μg) was treated with DNase I at room temperature for 15 min and then reverse-transcribed at 50°C for 50 min in a final volume of 20 μl of 1× first strand buffer (50 mM Tris-HCl, pH 8.0, 75 mM KCl, and 3 mM $MgCl_2$) containing random hexamer primers, 50 units of RNaseOut recombinant ribonuclease inhibitor, and 50 units of Superscript III. The resulting cDNAs were treated by 50 units of RNase H at 37°C for 20 min and diluted five times in RNase-free H_2O before quantitative real-time PCR as described below.

Quantitative Real-Time PCR. Most of the real-time PCR primers used in this study for quantifying mRNAs of UGT enzymes have been described previously (Congiu et al., 2002), including both forward and reverse primers for 18S rRNA and UGTs 1A1, 1A4, 1A6, 1A9, 2B4, 2B7, 2B10, 2B11, 2B15, and 2B17, and the reverse primers for UGTs 1A10 and 2B28. The forward primer for UGT1A10 was described elsewhere by (Strassburg et al., 1997). Primers for UGTs 1A3, 1A7, and 1A8, and the forward primer for UGT2B28 were designed in this study as shown in Table 1. A set of gene-specific reference templates were prepared to generate standard curves for quantification. Templates containing full-length target cDNAs included pEF-IRES-derived templates (UGTs 1A3, 1A7, 1A8, and 1A10), a PBS-derived template for UGT1A4, and a pCR-blunt-template for UGT2B28. The templates for the remaining target genes (18S rRNA, UGTs 1A1, 1A6, 1A9, 2B4, 2B7, 2B10, 2B11, 2B15, and 2B17) were all PCR-blunt-derived plasmids containing a single copy of the gene-specific RT-PCR product amplified from cDNA samples as described above. All primers were synthesized by Sigma-Genosys (Castle Hill, NSW, Australia).

Real-time PCR was performed using a RotorGene 3000 instrument (Corbett Research, NSW, Australia) in 20 μl of 1× QuantiTect SYBR Green PCR master mix (Sigma-Aldrich) containing 2 μl (~40 ng) of each aforementioned cDNA sample and a pair of gene-specific primers (~500 nM for each primer). The amplification conditions consisted of an initial activation step of 95°C for 15 min, and 40 cycles of 95°C for 10 s, 56 to 60°C for 15 s, and 72°C for 20 s. Data were obtained during the 72°C extension phase of each cycle and analyzed by the program RotorGene 6.1 (Corbett Research, Mortlake, NSW, Australia). Each sample was amplified in duplicate and the resultant mean values were used for analysis. Four serial 10×-diluted samples containing known copy numbers (e.g., 6000, 600, 60, and 6 for all UGTs) of gene-specific reference templates were included in each real-time PCR to generate a standard calibration curve, to calculate copy numbers of target transcripts in the samples amplified in the same run. Copy numbers of 18S rRNA transcripts were used as a reference to normalize the amount of total RNA amplified in each reaction. Quantification of mRNA expression was expressed as the relative copy number of each target transcript per 10^3 or 10^9 copies of 18S rRNA transcript.

Construction of Luciferase Reporter Constructs. For the sake of simplicity, the "A" of the initiation codon (ATG) was num-

bered + 1 to describe the positions of nucleotides in the promoter throughout this article. The fragment from nucleotides −3 to −2716 of the *UGT2B15* promoter was amplified from human genomic DNA (Roche Diagnostics, Indianapolis, IN) by PCR with primers 2B15-2716For and 2B15-3Rev (Table 1) and ligated into the KpnI and MluI sites of pGL3-basic vector to generate the luciferase reporter construct (2B15-2716/−3Luc). The promoter region from nucleotides −3 to −747 was amplified from this construct with primers 2B15-747For and 2B15-3Rev (the common reverse primer) (Table 1) and cloned into the same position of pGL3-basic vector to create the construct 2B15-747/−3Luc. Constructs of 2B15-705/−3Luc, 2B15-595/−3Luc, 2B15-556/−3Luc, 2B15-458/−3Luc, 2B15-412/−3Luc, 2B15-253/

TABLE 1

Primers used in this study for promoter cloning, mutagenesis, real-time PCR, EMSAs, and ChIP assays

PCR primers are numbered relative to the adenine base of the initiator codon (ATG), which is assigned as +1. Incorporated restriction sites of both MulI (ACGCGT) and KpnI (GGTACC) are underlined. Oligonucleotides are the same for both mutagenesis and EMSAs. Mutated sequences are highlighted in bold.

Primer	Nucleotide Sequence (5′ to 3′)
PCR and cloning	
2B15-54For	AGCCATGGTACCGAGAAATGACAGAAAG
2B15-101For	AGCCATGGTACCTAGCAGTTATATTTTAAC
2B15-154For	AGCCATGGTACCTCCTTGGCATGCACCTATTC
2B15-202For	AGCCATGGTACCCACCAAACACACTAAAA
2B15-253For	AGCCATGGTACCCTAGGTCATAAAAATTA
2B15-310For	AGCCATGGTACCGCCACTGTTCTTAACAGT
2B15-361For	AGCCATGGTACCTACTTCTTCTCTCTATGTC
2B15-412For	AGCCATGGTACCAAGACATTACTTGCACCACGA
2B15-458For	AGCCATGGTACCTTGGTGAGTCATATGGC
2B15-556For	AGCCATGGTACCGAGGCTATTGTATAGAATC
2B15-595For	AGCCATGGTACCTAGGGTAGGATGGATG
2B15-705For	AGCCATGGTACCAATCTAGTCCTGCATCC
2B15-747For	AGCCATGGTACCTTCACAATGCAAGCCTCTG
2B15-2716For	AAATCTGGGTACCACATAATGCCTGCACT
2B15-3Rev	AGAACGCGTGGTCTTATGCAATGCTTCTT
Site-directed mutagenesis/EMSA	
5′AP-1wt	GTACACACTAATTGGTGAGTCATATGGTATATG
5′AP-1m	GTACACACTAATTGG**CAGAG**CATATGGTATATG
3′AP-1wt[a]*	GGTATATGAATTATGTGTCAACAAAGTTTTAGAAGAC
3′AP-1m[a]*	GGTATATGAATTA**CAGAG**CAACAAAGTTTTAGAAGAC
3′AP-1wt[b]†	TATGAATTATGTGTCAACAAAGTTT
3′AP-1m[b]†	TATGAATTA**CAGAG**CAACAAAGTTT
3′EREhwt	AAATAAATATGAGGTCATCAATCTTTTGTTG
3′EREhm	AAATAAATATGA**AAAAA**TCAATCTTTTGTTG
5′EREhwt	CTTACATATTCTAGGTCATAAAAATTATTG
5′EREhm	CTTACATATTCTA**TTTTT**TAAAAATTATTG
EREfwt	CTCTCTATGTCAAGGGCACCGAACAGGC
EREfm	CTTCTTCTCTCTA**AAAAG**AGGGCACCGAAC
X. laevis VitellogeninA2 vitERE	AAAGTCAGGTCACAGTGACCTGATCAAAG
Quantitative real-time PCR	
c-Fos-For	TGATGACCTGGGCTTCCCAG
c-Fos-Rev	CAAAGGGCTCGGTCTTCAGC
c-Jun-For	CTTCAACCCAGGCGCGCTGAGCA
c-Jun-Rev	GTCTGAGGCTCCTCCTTCAGGGCCT
ERα-For	TTCGGCTCCAACGGCCTGGGGGGTTT
ERα-Rev	GGTACTGGCCAATCTTTCTCTGCCACCCT
Fra-2-For	TAGATATGCCTGGCTCAGGCAGTGCA
Fra-2-Rev	TCTTGATCACGCCAGGTCTTGGGA
18S rRNA-For	CGATGCTCTTAGCTGAGTGT
18S rRNA-Rev	GGTCCAAGAATTTCACCTCT
1A3-For	ATGGCAATGTTGAACAATATG
1A3-Rev	GGTCTGAATTGGTTGTTAGTAATC
1A7-For	TGGCTCGTGCAGGGTGGACTG
1A7-Rev	TTCGCAATGGTGCCGTCCAGC
1A8-For	CTGCTGACCTGTGGCTTTGCT
1A8-Rev	CCATTGAGCATCGGCGAAAT
2B28-For	TCTTTTTGATCCCAATGACGCATT
β-Actin-For	CTGGCGGCACCACCATGTACCCT
β-Actin-Rev	GGAGGGGCCGACTCGTCATACT
ChIP assay	
2B15-ChipF1	TGCCGTTTGAGTTGTATAATTACTTCTTC
2B15-ChipR1	GAATAGGTGCATGCCAAGGAGACC
2B15-ChipF2	GGGGGGTTAGAGGCTATTGTATAGA
2B15-ChipR2	GAATATGTAAGTAACCTGTCTTATGT
2B15-ChipR3	TTAATATCGTGGTGCAAGTAATGTCTTC
2B15-ChipF3	GAGTGGGGGGTTAGAGGCTATTGTATAG
HCG3-ChipF	ATGGTGGACTACTACGAGGT
HCG3-ChipR	CACCTGCTTGAATCTCCTCT
TFF1/pS2-For	GGCCATCTCTCACTATGAATCACTTCTGC
TFF1/ps2-Rev	GGCAGGCTCTGTTTGCTTAAAGAGCG

F, forward; For, forward; R, reverse; Rev, reverse; EREhwt, ERE wild-type half-site; EREhm, ERE mutant half-site; EREfwt, imperfect ERE full site; EREfm, ERE mutant full site.

* Used for the proximal AP-1 site in mutagenesis.

† Used for the proximal AP-1 site in EMSAs.

−3Luc, 2B15-202/−3Luc, 2B15-154/−3Luc, and 2B15-54/−3Luc were prepared in a similar manner using the construct 2B15-747/−3Luc as a template and specific primers as detailed in Table 1. The promoter sequences of all reporter constructs were confirmed by sequencing.

Mutagenesis of Putative AP-1 and ERE Binding Sites in Reporter Constructs. Mutagenesis was carried out using the QuikChange site-directed mutagenesis kit (Stratagene, La Jolla, CA) and complementary pairs of oligonucleotide primers with the desired mutation(s) in the middle of the primer. The sense sequences of the primers are detailed in Table 1. The mutation from "TGAGTCA" to "CAGAGCA" at the 5′-AP-1 site with the primer 5′AP-1m and the mutation from "TGTGTCA" to "CAGAGCA" at the 3′-AP-1 site using the primer 3′AP-1m[a] were separately or simultaneously introduced into three different UGT2B15 promoter constructs: 2B15-458/−3Luc (Fig. 3B, MT-6, MT-7, and MT-8), 2B15-747/−3Luc (Fig. 3B, MT-9, MT-10, and MT-11), and 2B15-2716/−3Luc (Fig. 3B, MT-12, MT-13, and MT-14). The 3′-ERE half-site was mutated from "GGTCA" to "AAAAA" in both 2B15-412/−3Luc (Fig. 3B, MT-1) and 2B15-458/−3Luc (Fig. 3B, MT-3) using the primer 3′EREhm. The imperfect ERE full-site mutation from "TGTCAaggGCACC" to "AAAAGaggGCACC" was introduced into both 2B15-412/−3Luc (Fig. 3B, MT-2) and 2B15-458/−3Luc (Fig. 3B, MT-5) with the primer EREfm. The 5′-ERE half-site of "GGTCA" was changed to "TTTTT" in 2B15-458/−3Luc (Fig. 3B, MT-4) using the primer 5′EREhm. The three sites, 3′-AP-1, 5′-AP-1, and the 3′-ERE half-site were all mutated in MT-15 (Fig. 3B) by introducing a mutation at the 3′-ERE half-site in the mutant MT-8 (Fig. 3B). A mutation was created in the imperfect ERE full site in MT-8 to generate the mutant MT-16 (Fig. 3B), which contained mutations at both AP-1 sites and the imperfect ERE full-site. In addition, the proximal AP-1 site (starting at nucleotide −372) of the *UGT2B17* promoter in the construct 2B17-650/+42Luc was mutated using primer 3′AP-1m[a] to create the mutant 2B17-650/+42LucMut (Fig. 9B). The identities of all mutants were verified by sequencing.

Transient Transfection. MCF-7 cells were plated into 96-well plates at a density of 2.5×10^4 cells/well in 200 μl of phenol red-free RPMI 1640 medium with 6% FBS. After 24 h, cells were washed twice using 1× PBS before transfections. Transfections were carried out in 50 μl of phenol red-free RPMI 1640 medium without serum using 100 ng of each reporter construct with (cotransfection) or without 2.5 ng of ERα expression plasmid HEGO/pSG5 and 0.4 μl of LipofectAMINE 2000 per transfection according to the manufacturer's instructions (Invitrogen). After 5 h, the transfection mix was removed, and cells were treated with either 10 nM 17β-estradiol or 0.1% ethanol (vehicle). Forty hours after treatment, cells were harvested in 100 μl of 1× passive lysis buffer and assayed for firefly luciferase activities using the Luciferase Reporter Assay system (Promega, Madison, WI) and a Packard TopCount luminescence and scintillation counter (PerkinElmer Life and Analytical Sciences, Waltham, MA). The plasmid HEGO/pSG5 contained the full cDNA sequence of human estrogen receptor alpha cloned into the pSG5 vector and was a kind gift from Dr Amelia Peters (University of Adelaide, Adelaide, SA, Australia).

Electrophoretic Mobility Shift and Supershift Assays. Nuclear extracts were prepared from MCF-7 cells as reported previously (Gardner-Stephen et al., 2005) except that cells were preincubated for 6 days in phenol red-free RPMI 1640 medium supplemented with 5% DCC-stripped FBS and treated for a further 24 h with 10 nM 17β-estradiol. Recombinant human ERα was prepared with the ERα expression plasmid HEGO/pSG5 using the TnT Quick Coupled Transcription/Translation kit according to the manufacturer's instructions (Promega). The probes for electrophoretic mobility shift assays (EMSAs) were generated with the same primers as used in mutagenesis, except that a different pair of primers was designed for the probe analyzing the proximal AP-1 site (Table 1). In brief, probes were prepared by annealing complementary sense and antisense oligonucleotides, followed by end-labeling with [γ-^{32}P]ATP (PerkinElmer Life and Analytical Sciences) using T4 polynucleotide kinase (New England Biolabs, Ipswich, MA) and purification through G25 columns (GE Healthcare Australia Pty Ltd., Rydalmere, NSW, Australia). The EMSA reactions consisted of 1 μg of poly(dI-dC) (Sigma) and either 5 μg of MCF-7 nuclear extract or 1 μl of in vitro-transcribed/translated ERα protein in a 15-μl buffer containing 25 mM Tris-HCl, pH 7.6, 100 mM KCl, 5 mM $MgCl_2$, 0.5 mM EDTA, and 10% glycerol. After incubation on ice for 10 min, 50,000 cpm of probe (~1 ng) was added, and the reaction was incubated at room temperature for a further 30 min. For competitive assays, unlabeled wild-type or mutated probes were added into the reaction in a 10 to 100 M excess of labeled probe before the initial 10-min incubation on ice. For supershift assays, 2 μg of antibody (~1 μl) was added immediately after the addition of labeled probes. DNA-protein complexes were resolved in 0.5× Tris borate-EDTA on 4% nondenaturing polyacrylamide gels. The gels were dried and exposed to X-ray films followed by autoradiography. All antibodies were purchased from Santa Cruz Biotechnology (Santa Cruz, CA), including anti-ERα (HC-20), anti-c-fos (H125), anti-c-fos (K-25), anti-c-fos (4), anti-Fra-1 (N-17), anti-Fra-2 (L-15), FosB (102), anti-c-Jun (N), and anti-c-Jun (D). As shown in Fig. 4, the two specific anti-c-Fos antibodies, H125 and 4, were designated Ab_c-Fos1 and Ab_c-Fos2, respectively. The anti c-fos (K-25) was designated as Ab_Fos family because it recognizes all Fos family members, whereas the anti-c-Jun (D) recognizes all Jun family members, so it was designated Ab_Jun-family.

siRNA Knockdown Experiments. siGENOME SMARTpool siRNAs were purchased from Dharmacon RNAi Technologies (Lafayette, CO), including siRNAs directed against ERα, c-Jun, and Fra-2, and the scrambled siRNA (nontargeting siRNA pool 1) as a negative control. MCF-7 cells precultured in phenol red-free RPMI 1640 medium supplemented with 5% DCC-stripped FBS for 4 days were plated into six-well plates at a density of 5×10^5 cells per well in 1.5 ml of fresh medium containing 8 μl of LipofectAMINE 2000 (Invitrogen) and 100 nM target siRNA. Five hours after transfection, the medium was changed and cells were cultured in fresh phenol red-free RPMI supplemented with 5% DCC-stripped FBS. Forty-eight hours after transfection, cells were treated with 10 nM 17β-estradiol for a

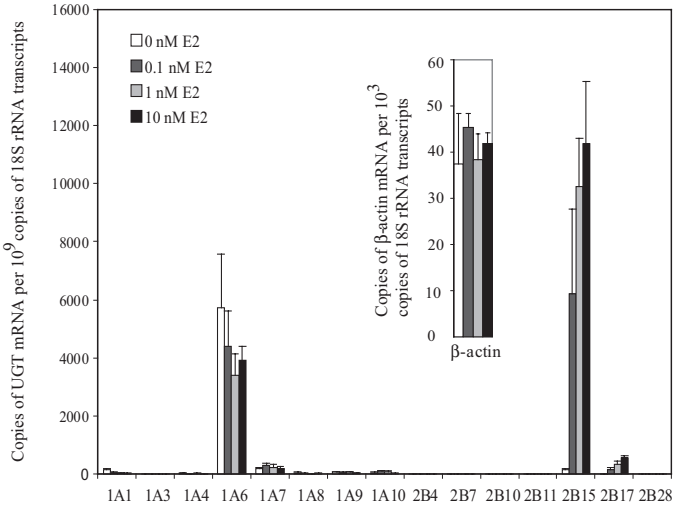

Fig. 1. 17-β Estradiol elevates UGT2B15 and UGT2B17 mRNA levels in MCF-7 cells. MCF-7 cells preincubated for 6 days in phenol red-free RPMI 1640 medium containing 5% DCC-stripped FBS were treated with either 17β-estradiol (E2) at three different concentrations (0.1, 1, or 10 nM) or 0.1% ethanol (vehicle) for 24 h. Total RNA was extracted and reverse-transcribed to generate cDNA, followed by quantitative real-time PCR to calculate the copy numbers of target transcripts as described under *Materials and Methods*. Relative expression levels were calculated as copies of each target transcript per 10^9 copies (for all UGTs) or 10^3 copies (for β-actin) of 18S rRNA transcripts. Data shown are from a representative experiment performed in triplicate, the error bars indicating 1 S.D. Inset, data for β-actin.

further 24 h and then harvested for assessing the mRNA levels of each target gene by quantitative real time RT-PCR with gene-specific primers (Table 1).

Chromatin Immunoprecipitation Assay. MCF-7 cells were cultured for 6 days in phenol red-free RPMI containing 6% DCC-stripped FBS and treated with either 10 nM 17β-estradiol or 0.1% ethanol (vehicle) for 2 h or 24 h. Cross-linking was achieved by treating the cells with 1% formaldehyde at 37°C for 30 min and subsequently quenched by incubating the cells at 37°C for 10 min in 1× PBS solution containing 125 mM glycine. Cells from three T175 flasks (~90% confluence) were washed twice with 1× PBS and lysed in 10 ml of buffer (15 mM Tris-HCl, pH 8.0, 1% Nonidet P40, 0.5 mM EGTA, 15 mM NaCl, 60 mM KCl, 300 mM sucrose, and 0.5 mM β-mercaptoethanol) containing 1× protease inhibitor mixture (Roche). The resultant lysates were incubated on ice for 10 min, and nuclei pellets were colleted by centrifugation at 4000 rpm at 4°C for 10 min. The pellets were resuspended in 1.5 ml of nuclear lysis buffer (1% SDS, 10 mM EDTA, 0.5 mM phenylmethylsulfonyl fluoride, and 50 mM Tris-HCl, pH 8.0) containing 1× protease inhibitor mixture (Roche), and incubated on ice for at least 15 min, followed by sonication to yield fragments ranging in size from 500 to 1200 bp. Supernatants of the sonicated products were collected by centrifugation at 14,000 rpm for 10 min at 4°C, diluted six times in dilution buffer (16.7 mM Tris-HCl, pH 8.0, 0.01% SDS, 1% Triton X-100, 1.2 mM EDTA, 150 mM NaCl, and 1× protease inhibitor mixture), and then immuno-precleared at 4°C for 2 h with 300 μl of 50% Protein A Sepharose CL-4B (GE Healthcare) containing 50 μg of salmon sperm DNA and 20 μg of BSA. The precleared chromatin samples were recovered after centrifugation at 4°C for 1 min, and ~0.8 ml aliquots saved as input DNA or subjected to immunoprecipitation at 4°C overnight with 10 μg of each antibody, or equivalent amounts of preimmune IgG serum (designated as IgG) as a negative control. After antibody treatment, 100 μl of 50% protein A Sepharose CL-4B containing 17 μg of salmon sperm DNA and 7 μg of BSA was added to each sample, and the incubation was continued for another 2 h. The precipitates were collected by centrifugation as described above and then washed sequentially for 1 min, twice in dilution buffer, high salt buffer (16.7 mM Tris-HCl, pH 8.0, 0.01% SDS, 1% Triton X-100, 1.2 mM EDTA, and 500 mM NaCl), LiCl buffer (16.7 mM Tris-HCl, pH 8.0, 0.01% SDS, 1% Triton X-100, 1.2 mM EDTA, and 250 mM LiCl), and Tris-EDTA buffer (16.7 mM Tris-HCl, pH 8.0, and 1.2 mM EDTA). The protein-DNA complexes were eluted from the beads in 200 μl of elution buffer (1% SDS and 0.1 M $NaHCO_3$). Cross-linking was reversed by heating the eluates at 65°C overnight. The supernatants containing the precipitated DNA were collected after centrifugation and digested with proteinase K at 37°C for 6 h, followed by phenol-chloroform extraction and ethanol precipitation. The DNA pellets were resuspended in 50 μl of Tris-EDTA buffer. Quantitative real-time PCR was performed using 2 μl of each of the resultant DNA samples and primers (Table 1), which were specific to the *UGT2B15* promoter, the coding region of the *HCG3* gene (NM_001001394) on chromosome 2 (2q37) as a reference gene for data normalization, or the promoter of the *trefoil factor 1* gene (*pS2*/*TFF1*) as a positive control. Data obtained from the *HCG3* gene were used to normalize the starting amounts of the immunoprecipitated DNA samples seeded in each PCR reaction.

Phorbol 12-Myristate 13-Acetate Treatment and Analysis of Gene Expression. Phorbol 12-myristate 13-acetate (PMA; 100 μM; Sigma) was prepared with ethanol as a stock solution. MCF-7 cells were preincubated for 3 days in phenol red-free RPMI 1640 medium with 6% DCC-stripped FBS and then plated into six-well plates in the same medium. Three days after plating, cells were treated with 0.1% ethanol (vehicle), 100 nM PMA for 6 h, 10 nM 17β-estradiol for 24 h, or a combination of 10 nM 17β-estradiol for 24 h and 100 nM PMA for 6 h. After treatment, cells were harvested, total RNA was extracted, and target mRNAs were quantified by quantitative real-time RT-PCR as above.

Results

17β-Estradiol Induces Expression of *UGT2B15* and *UGT2B17* in MCF-7 Cells. A recent study identified the human *UGT2B15* gene as an estrogen-responsive gene in MCF-7 breast cancer cells (Harrington et al., 2006). To determine whether estrogens also regulate other *UGT* genes, we treated MCF-7 cells for 24 h with 0.1% ethanol (vehicle) or 17β-estradiol at three different concentrations (0.1, 1, and 10 nM), and then quantified the mRNA levels of eight UGT1A and seven UGT2B enzymes by quantitative real-time RT-PCR.

Vehicle-treated MCF-7 cells contained high levels of UGT1A6 mRNA, low levels of UGTs 1A1, 1A4, 1A7, 1A8, 1A9, 1A10, and 2B15 mRNA, and barely detectable levels of UGT2B17 mRNA. The mRNA levels for UGTs 1A3, 2B4, 2B7, 2B10, 2B11, and 2B28 were below the detectable level (Fig. 1). As expected, treatment of MCF-7 cells with 17β-estradiol at all three concentrations (0.1, 1, and 10 nM) elevated UGT2B15 mRNA levels by approximately 39-, 63-, and 72-fold, respectively, compared with that in the absence of 17β-estradiol (Fig. 1). We were surprised to find that treating MCF-7 cells with 0.1 nM 17β-estradiol also increased UGT2B17 mRNA levels by 21-fold compared with that in vehicle-treated cells. This 17β-estradiol-mediated induction was further enhanced by 2- and 3.7-fold in cells treated with

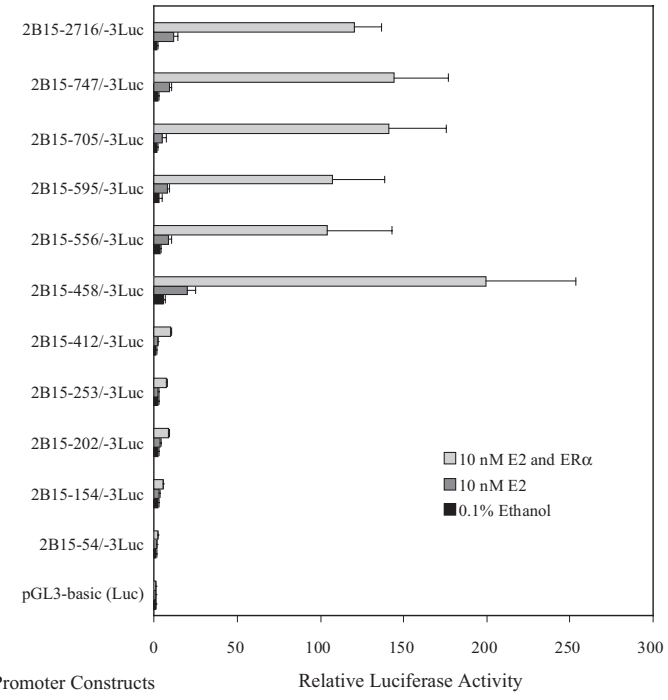

Fig. 2. Deletion analysis of the *UGT2B15* promoter in MCF-7 cells indicates the presence of *cis*-activating elements responsive to 17β-estradiol. A series of luciferase reporter constructs carrying varying lengths of the *UGT2B15* proximal promoter is shown on the left. Transient transfections with MCF-7 cells were carried out using 100 ng of each promoter construct with or without 2.5 ng of ERα expression plasmid. Five hours after transfection, cells were treated with either 10 nM 17β-estradiol (E2) or 0.1% ethanol (vehicle). Forty hours after treatment, cells were harvested and assayed for firefly luciferase activity as described under *Materials and Methods*. The relative luciferase activities of *UGT2B15* promoter constructs are expressed as -fold induction over that of the promoterless pGL3-basic vector (set at a value of 1) for the respective conditions, as indicated by "0.1% ethanol", "10 nM E2," and "10 nM E2/ERα," respectively. Data shown are from a representative experiment performed in triplicate, error bars representing 1 S.D.


A
WT
-454TGAGTCA
-431TGTGTCA
-346TGTCAaggGCACC
-250GGTCA
-176GGTCA
5'
5'-AP-1
3'-AP-1
Imperfect ERE site
5'-ERE half-site
3'-ERE half-site
ATG
MT
-454CAGAGCA
-431CAGAGCA
-346AAAAGaggGCACC
-250TTTTT
-176AAAAA

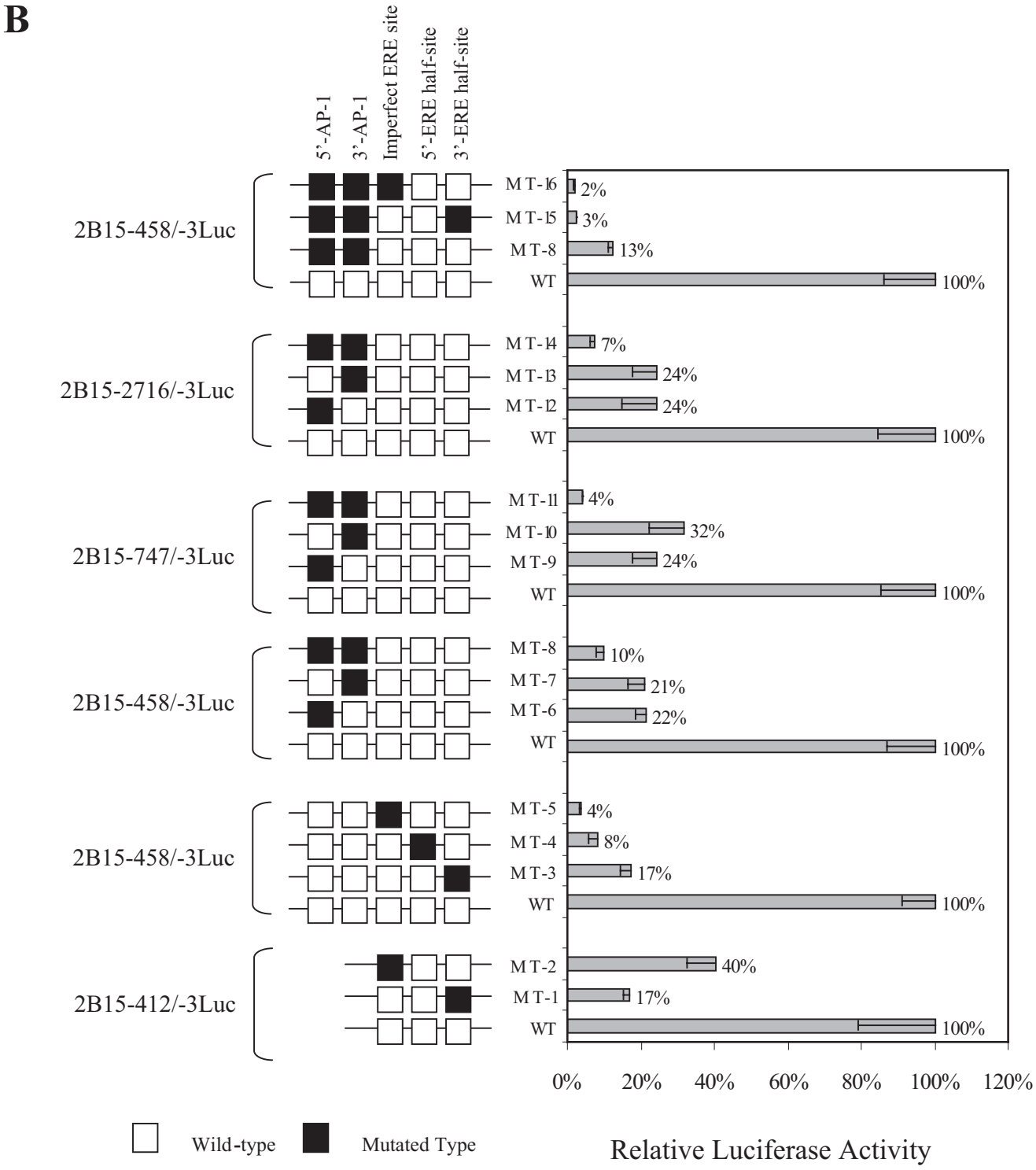
B
5'-AP-1
3'-AP-1
Imperfect ERE site
5'-ERE half-site
3'-ERE half-site
2B15-458/-3Luc
MT-16
2%
MT-15
3%
MT-8
13%
WT
100%
2B15-2716/-3Luc
MT-14
7%
MT-13
24%
MT-12
24%
WT
100%
2B15-747/-3Luc
MT-11
4%
MT-10
32%
MT-9
24%
WT
100%
2B15-458/-3Luc
MT-8
10%
MT-7
21%
MT-6
22%
WT
100%
2B15-458/-3Luc
MT-5
4%
MT-4
8%
MT-3
17%
WT
100%
2B15-412/-3Luc
MT-2
40%
MT-1
17%
WT
100%
0%
20%
40%
60%
80%
100%
120%
Wild-type
Mutated Type
Relative Luciferase Activity

Fig. 3.

17β-estradiol at 1 and 10 nM, respectively (Fig. 1). However, the levels of UGT2B17 mRNA were much lower than those of UGT2B15, in both the presence and the absence of 17β-estradiol (Fig. 1). Treatment with 17β-estradiol (0.1–10 nM) had little effect on the mRNA levels of the remaining 13 UGT enzymes and β-actin, a house-keeping gene used as an internal control (Fig. 1, inset).

Overall, it seems that not only *UGT2B15* but also *UGT2B17* are estrogen-targeted genes, because both are upregulated by 17β-estradiol in a dose-dependent manner in MCF-7 cells. Because *UGT2B15* expression was much higher than *UGT2B17* expression, this study focused on *UGT2B15* in an attempt to define the mechanism underlying this selective 17β-estradiol-induced *UGT* expression.

The Proximal Promoter of the *UGT2B15* Gene Responds to 17β-Estradiol through an Estrogen Response Unit Containing Multiple AP-1 and Estrogen Response Elements. To determine whether induction of *UGT2B15* expression by 17β-estradiol is mediated through the *UGT2B15* promoter, a series of proximal promoter fragments of various lengths were incorporated into the luciferase gene reporter pGL3-basic vector and tested for their capacity to drive transcription in MCF-7 cells in transient transfection experiments.

In the absence of 17β-estradiol, the *UGT2B15* promoter constructs tested gave very low basal activities of only 2- to 5-fold more than that of the negative control, the promoterless pGL3-basic vector (Fig. 2). Stimulation by 17β-estradiol (10 nM) had small effects on the activities of promoters ≤412 bp long, whereas the activities of promoters ≥458 bp long were markedly increased, with the construct 2B15-458/−3Luc giving the highest activity of approximately 18-fold compared with that of pGL3-basic. Treatment by 17β-estradiol in combination with transfected ERα further increased the activities of promoters ≥458 bp long. The activity of construct 2B15-458/−3Luc was 200-fold greater than that of the control pGL3-basic vector. This was equivalent to a 36-fold induction in promoter activity over that of the controls treated with vehicle alone. These results suggested the presence of estrogen-responsive *cis*-activating element(s) in the promoter region from nucleotides −412 to −458. Sequence analysis of this 47-bp region showed two putative AP-1 sites (separated by 16 bp); one consensus site from nucleotides −448 to −454 (5′-TGAGTCA-3′, designated 5′-AP-1) and the other from nucleotides −425 to −431 (5′-TGTGTCA-3′, designated 3′-AP-1). The latter deviates from the consensus by only one nucleotide (Fig. 3A).

We mutated the two AP-1 sites separately or together in three promoter constructs of varying lengths: 2B15-458/−3Luc, 2B15-747/−3Luc, and 2B15-2716/−3Luc (Fig. 3B). We examined the effects of these mutations on 17β-estradiol/ERα-activated promoter activities. Compared with activity (set at a value of 100%) of the wild-type constructs, activities were decreased to 21 to 32% for mutants carrying mutations at either the 5′-AP-1 site (MT-6, MT-9, and MT-12) or the 3′-AP-1 site (MT-7, MT-10, and MT-13) and, furthermore, to approximately 4 to 10% for mutants with mutations at both AP-1 sites (MT-8, MT-11, and MT-14). These results demonstrate the importance of both AP-1 sites in mediating 17β-estradiol-stimulated *UGT2B15* expression. To the best of our knowledge, this is the first evidence that a native promoter responds to 17β-estradiol via two adjacent AP-1 binding sites.

The activities of constructs carrying a promoter region between nucleotides −154 and −412 were also moderately enhanced by 5- to 10-fold over the control pGL3-basic vector after 17β-estradiol treatment and transfection of ERα (Fig. 2). Construct 2B15-412/−3Luc gave a moderate induction of 7-fold compared with that of the vehicle-treated controls. These results imply that additional estrogen-inducible elements might also be present in the promoter region from nucleotides −154 to −412. As shown in Fig. 3A, sequence analysis of this region revealed one imperfect ERE site between nucleotides −334 and −346 (5′-TGTCAaggGCACC-3′) (designated Imperfect ERE site) and two putative ERE half-sites from nucleotides −246 to −250 (5′-GGTCA-3′) (5′-ERE half-site) and from −172 to −176 (5′-GGTCA-3′) (3′-ERE half-site), respectively. The importance of these sites for 17β-estradiol/ERα-dependent induction was also investigated by mutagenesis. Compared with the wild-type constructs, mutations of the 3′-ERE half-site in both constructs 2B15-412/−3Luc (Fig. 3B, MT-1) and 2B15-458/−3Luc (Fig. 3B, MT-3) decreased the promoter activity to a similar level of ~17%. When the 5′-ERE half-site was mutated in construct 2B15-458/−3Luc (Fig. 3B, MT-4), promoter activity was significantly reduced to approximately 8%. Mutation of the imperfect ERE site resulted in a 60% reduction in promoter activity of construct 2B15-412/−3Luc (Fig. 3B, MT-2) and almost abolished the activity of construct 2B15-458/−3Luc (Fig. 3B, MT-5). Collectively, our data clearly demonstrate that these three ERE/half-EREs respond cooperatively to 17β-estradiol. Given their close proximity to each other (only 164 bp apart), they probably act as a cooperative unit, as was observed with the *X. laevis vitellogenin B1* and *B2* genes and the chicken ovalbumin gene (Klein-Hitpass et al., 1988; Kato et al., 1992).

In addition, although mutations in both AP-1 sites reduced 17β-estradiol/ERα-activated promoter activities to approximately 10 to 13% that of the unmutated construct (Fig. 3B, MT-8), further mutations in the 3′-ERE half-site and imperfect ERE reduced activity to only 2 to 3% (Fig. 3B, MT-15 and MT-16). Thus it seems that the 2 AP-1 and 2 ERE-half sites, as well as the imperfect ERE of the *UGT2B15* promoter, act synergistically in response to 17β-estradiol and hence constitute an estrogen response unit.

Fig. 3. Mutational analysis of the *UGT2B15* proximal promoter identifies five functional *cis*-activating elements responsible for estrogen-inducibility. A, a schematic depiction of the five putative *cis*-activating elements in the *UGT2B15* proximal promoter from nucleotides −3 to −485, including two AP-1 sites beginning at nucleotides −454 (5′-AP-1) and −431 (3′-AP-1), two ERE half-sites at −250 bp (5′-ERE half-site) and −176 bp (3′-ERE half-site), and an imperfectly palindromic ERE site at −346 bp. The sequences at these sites (WT) and their mutations (MT) are shown. B, shown at the left are 16 mutated constructs of the *UGT2B15* proximal promoter with mutations at one or more of the aforementioned five putative sites indicated by black boxes. Transient transfections with MCF-7 cells were carried out using 100 ng of each promoter construct with 2.5 ng of ERα expression vector. Five hours after transfection, cells were treated with 10 nM 17β-estradiol in phenol red-free RPMI 1640 medium with 5% DCC-stripped FBS. Forty hours after treatment, cells were harvested and assayed for firefly luciferase activities as described under *Materials and Methods.* Data shown are representative experiments performed in triplicate with error bars representing 1 S.D. After normalizing to the promoterless pGL3-basic vector, the relative luciferase activities of the mutants are expressed as a percentage of that obtained from the relevant wild-type constructs (set at a value of 100%).

c-Jun and Fra-2 Bind to the Distal AP-1 Site in the *UGT2B15* Proximal Promoter. We next sought to use EMSAs to determine whether AP-1 factors bound to the two AP-1 sites within the *UGT2B15* promoter. AP-1 factors are leuzine-zipper-containing transcription factors of the Jun (c-Jun, JunB, and JunD) and Fos (c-Fos, FosB, Fra-1, and Fra-2) families. Members of the Jun family can form homodimers (e.g., c-Jun/c-Jun), whereas members of the Fos family only form heterodimers with Jun family members (e.g., c-Jun/c-Fos, c-Jun/Fra-2, and JunD/Fra-2) (Hess et al., 2004). To determine whether AP-1 proteins were able to bind to the distal AP-1 site (5′-AP-1), an EMSA was performed by incubating a probe encompassing the distal AP-1 site, corresponding to nucleotides from −469 to −437 of the *UGT2B15* promoter, with nuclear extracts from 17β-estradiol-stimulated MCF-7 cells. As shown in Fig. 4A, lane 1, three major complexes (labeled a, b, and c) were observed with the wild-type probe (Table 1, 5′AP-1wt). Mutation of this site from "TGAGTCA" to "CAGAGCA" (Table 1, 5′AP-1m) completely abolished the formation of complexes a and b and only slightly decreased the formation of complex c (lane 6). The formation of complexes a, b, and c were completely inhibited in the presence of a 10- to 100-fold molar excess of the unlabeled wild-type probe (lanes 2 and 3). However, only the formation of complex c was reduced by the addition of a 10- to 100-fold molar excess of the unlabeled mutated probe (lanes 4 and 5). These results indicate that proteins in MCF-7 nuclear extracts specifically bind to the distal AP-1 site, forming complexes a and b.

To identify the proteins in complexes a and b, supershift assays were performed using antibodies to ERα and members of the Jun and Fos families. The formation of complexes a and b was decreased by the addition of either the anti-Jun family antibody (Fig. 4, lane 12) or the anti-c-Jun antibody (lane 9), suggesting the presence of c-Jun in both complexes a and b. The anti-Fos family antibody inhibited the formation of complex b and resulted in the formation of a larger supershifted complex (labeled SS) (lane 11). The formation of complex b was also reduced by the addition of anti-Fra-2 antibody (lane 13), implying the presence of Fra-2 in complex b. Changes in the amounts of complexes a and b were not observed in a series of supershift assays with the addition of antibodies to ERα (lane 10) and other members of the Fos family, including Fra-1 (lane 14), FosB (lane 15), and c-Fos, with two different antibodies c-Fos1 (lane 8) and c-Fos2 (lane 16). Collectively, these results suggest that c-Jun and Fra-2 bind to the distal AP1 site in the *UGT2B15* promoter, mainly as AP-1 heterodimers c-Jun/Fra-2 in complex b or possibly homodimers c-Jun/c-Jun in complex a.

The above experiments were repeated with a probe encompassing the proximal AP-1 site (3′-AP-1) within the *UGT2B15* promoter. As shown in Fig. 4B, EMSAs with the

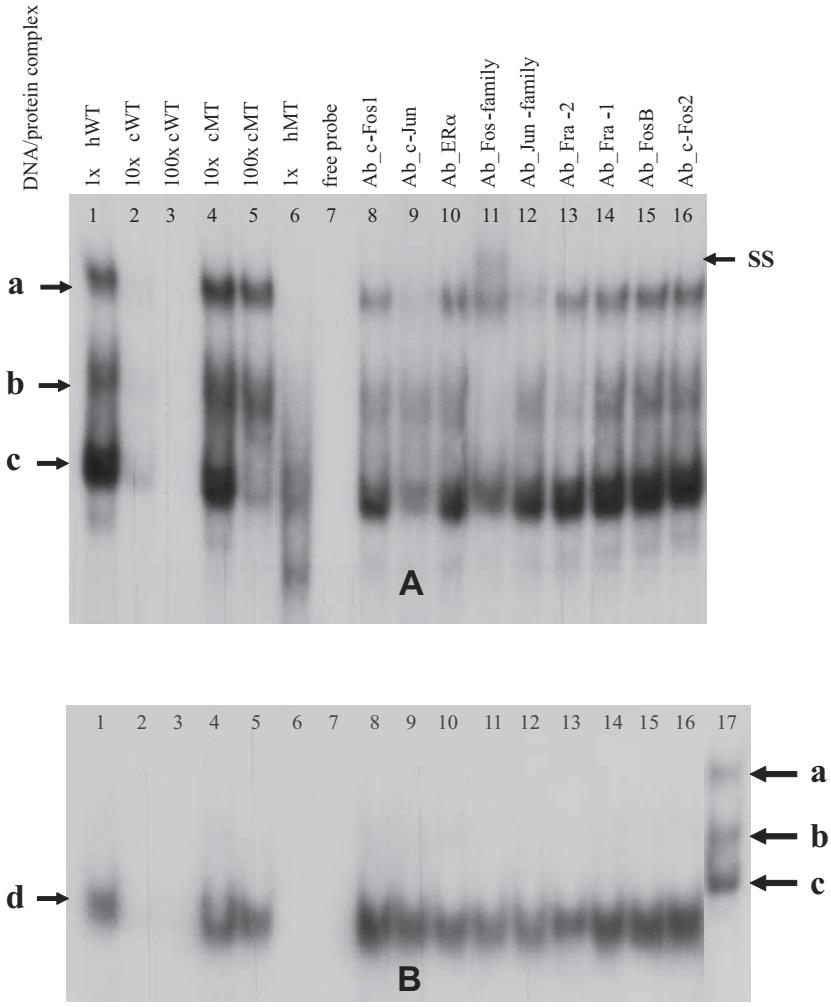

Fig. 4. c-Jun and Fra-2 bind to the distal AP-1 site in the *UGT2B15* promoter. EMSAs were performed with ^{32}P-end-labeled double-stranded oligonucleotide probes encompassing either the distal AP-1 site (5′-AP-1) (A) or the proximal AP-1 site (3′-AP-1) (B) of the *UGT2B15* promoter using 5 μg of MCF-7 nuclear extracts as described under *Materials and Methods.* In competition assays, unlabeled probes were added at a 10- (lanes 2 and 4) and 100-fold (lanes 3 and 5) molar excess of labeled probe before the addition of labeled probe. In supershift assays, 2 μg of antibodies (lanes 8–16 as indicated) were added immediately after the addition of labeled probe and incubated for 30 min at room temperature. Arrows indicate the major DNA/protein complexes pertinent to the 5′-AP-1 site (a, b, and c) and the 3′-AP-1 site (d), as well as the supershifted band (SS). Lane 17 is a replicate of lane 1 (A) to indicate the relative positions of these DNA/protein complexes. hWT, labeled probe; hMT, labeled mutated probe; cWT, unlabeled probe; cMT, unlabeled mutated probe.

labeled wild-type probe (Table 1, 3′AP-1wt[b]) showed a DNA/protein complex (labeled d) (lane 1), which migrated slightly faster than complex c, formed with the probe containing the distal AP-1 site (lane 17). We demonstrated that the formation of complex d was 3′-AP-1 site-specific by showing that it did not form on a labeled mutated probe (Table 1, 3′AP-1m[b] and Fig. 4B, lane 6) and that its formation was completely abolished in the presence of a 10- to 100-fold molar excess of the unlabeled wild type probe (lanes 2 and 3) but unaffected by a 10- to 100-fold molar excess of unlabeled mutated probe (lanes 4 and 5). However, despite extensive supershift assays with antibodies to ERα and members of the Jun and Fos families, the identities of the proteins in complex d could not be resolved as shown in Fig. 4B, lanes 8–16.

ERα Does Not Seem to Interact with Probes Containing Each of the Three Putative Imperfect and Half EREs of the *UGT2B15* Promoter in EMSAs. We further performed EMSAs with in vitro transcribed/translated recombinant human ERα proteins to determine whether ERα was able to bind to the imperfect ERE and two ERE half-sites within the *UGT2B15* ERU. As shown in Fig. 5A, the incubation of recombinant ERα with a probe containing the consensus ERE sequence (VitERE) of the *X. laevis Vitellogenin A2* gene resulted in major ERα/DNA complexes (labeled A, lane 2), which were supershifted (labeled SS) by the addition of the anti-ERα antibody (lane 3). However, these complexes were not observed with any of the probes containing the 3′-ERE half-site (lane 5), the 5′-ERE half-site (lane 8), and the imperfect ERE full-site (lane 11) (Table 1, 3′EREhwt, 5′EREhwt, EREfwt). We repeated these experiments with 17β-estradiol-stimulated MCF-7 nuclear extracts and observed similar results (data not shown). These results suggest that the binding of ERα might be too weak to be detected in standard EMSAs, which is in agreement with previous observations that the binding of ER to single ERE half-sites in vitro is 50- to 100-fold weaker than that to a perfect ERE (Tora et al., 1988; Kato et al., 1992).

We next performed competitive EMSAs to determine whether the binding of ERα to VitERE was competed with a 100-fold molar excess of unlabeled probes containing the individual imperfect ERE and ERE-half sites. As shown in Fig. 5B, the 3′-ERE half-site (lane 5) and the 5′-ERE half-site (lane 7) demonstrated significant abilities to compete for ERα binding to VitERE. The competition for ERα binding was abolished when the sequence (5′-GGTCA-3′) of each ERE half-site was mutated to be either 5′-TTTTT-3′ (Table 1, 5′EREhm) at the 5′-ERE half-site (lane 8) or 5′-AAAAA-3′ (Table 1, 3′EREhm) at the 3′-ERE half-site (lane 6), suggesting that such competition was specific to the intact ERE half-site. These results provide further evidence for a role of these two ERE half-sites in 17β-estradiol-stimulated UGT2B15 transcription.

The imperfect ERE full-site (Table 1, EREfwt) did not compete for ERα binding to VitERE (Fig. 5B, lane 9) despite evidence that mutation of this site almost completely abolished 17β-estradiol-induced activity of the *UGT2B15* promoter (Fig. 3B, MT-5). The reason for this is unknown, but is consistent with reports that an increasing number of natural and synthetic imperfect palindromic EREs are found to be estrogen-inducible in transient transfections but show very weak or no ERα binding in vitro as assayed by EMSAs (Tora et al., 1988; Kato et al., 1992; Klinge, 2001).

siRNA-Mediated Knockdown of ERα, Fra-2, and c-Jun Reduces the Capacity of 17β-Estradiol to Activate the *UGT2B15* Gene. Because mutagenesis implicated the

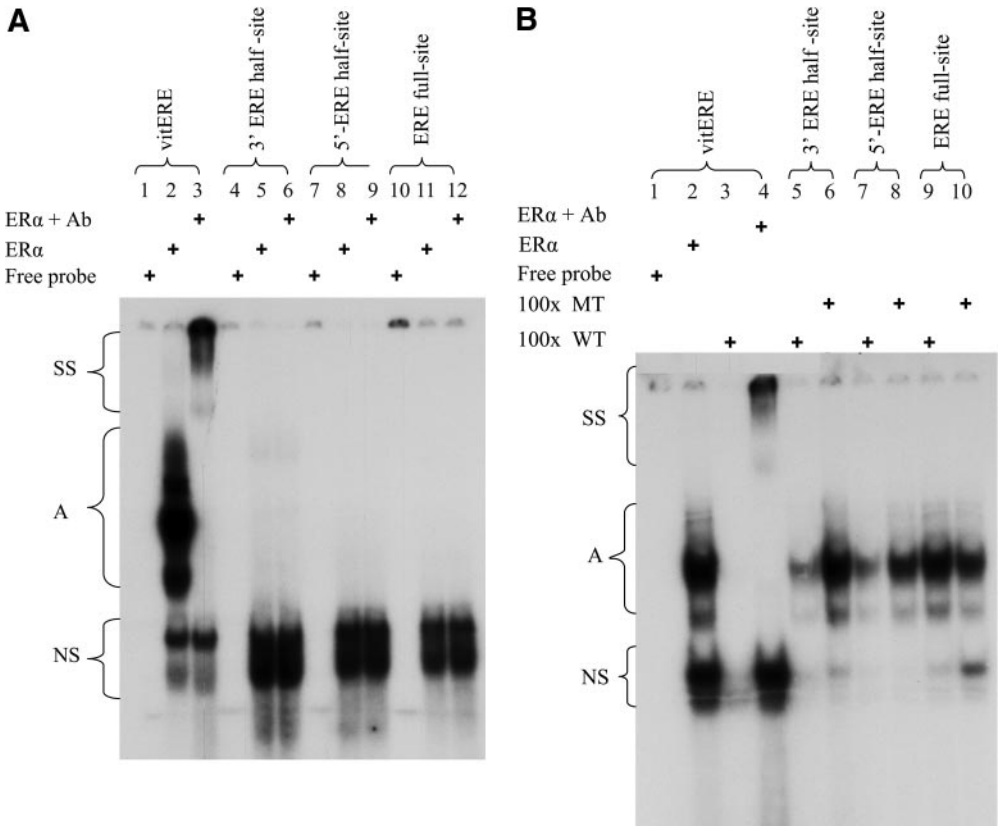

Fig. 5. A, recombinant human ERα does not bind to the two ERE half-sites and the imperfect ERE of the *UGT2B15* promoter. EMSAs were performed with 1 μl of in vitro transcribed/translated recombinant human ERα and 50,000 cpm (~1 ng) of ^{32}P-end-labeled double-stranded oligonucleotide probes encompassing either the consensus vitERE site of the *X. laevis Vitellogenin A2* gene or one of the three *UGT2B15* imperfect ERE and ERE half-sites (as indicated) as described under *Materials and Methods.* For supershift assays, 2 μg of anti-ERα antibody (lanes 3, 6, 9, and 12) were added immediately after the addition of labeled probe and incubated for 30 min at room temperature. The specifically bound ERα-DNA retarded complexes (A), the ERα antibody supershifted complexes (SS), and the nonspecifically retarded complexes (NS) are indicated with brackets. B, probes encompassing the ERE half-sites of the UGT2B15 proximal promoter significantly inhibit the formation of ERα/DNA complexes on the vitERE site of the *X. laevis Vitellogenin A2* gene promoter. EMSAs (lanes 2–10) with the vitERE probe were performed as above. For competition assays, unlabeled wild-type (WT; lanes 3, 5, 7, and 9) or mutated (MT, lanes 6, 8, and 10) probes were added at 100-fold molar excess before the addition of labeled probes.

involvement of an imperfect ERE, two ERE-half sites, and two AP-1 sites in the process of induction of *UGT2B15* promoter activity by 17β-estradiol, we sought to determine whether the relevant transcription factors that might bind to these sites are involved by altering their levels in MCF-7 cells using siRNA knockdown strategies. Because our EMSAs already demonstrated the binding of c-Jun and Fra-2 to the distal AP-1 site (Fig. 4A), we selected three siRNAs directed against c-Jun, Fra-2, and ERα and introduced them into MCF-7 cells by transient transfection, followed by measuring target mRNAs using quantitative real-time RT-PCR. As shown in Fig. 6A, treatment of MCF-7 cells with ERα siRNA successfully reduced the levels of endogenous ERα transcripts to 43% of that in cells treated with scrambled siRNAs. This reduction of ERα mRNA resulted in an approximately 10-fold decrease in UGT2B15 mRNA levels, whereas there was no effect on the mRNA levels of three other genes, including *GAPDH*, *UGT1A6*, and *Fra-2*. The levels of c-Jun mRNA were decreased by half, which is consistent with the reported activation of c-Jun transcription by estrogen (Weisz et al., 1990). As shown in Fig. 6B, down-regulation of c-Jun mRNA with siRNA to a level that was 51% that of control reduced UGT2B15 mRNA levels to 43% without significantly altering the mRNA levels of GAPDH, ERα, and Fra-2. c-Jun siRNA treatment also reduced the mRNA levels of UGT1A6 by approximately 3-fold, which is consistent with the proposed activation of the *UGT1A6* gene by AP-1 transcription factors (Heurtaux et al., 2006). As shown in Fig. 6C, down-regulation of Fra-2 with siRNA to a level that was 6% that of control decreased UGT2B15 mRNA levels by 5-fold, whereas the mRNA levels of three other genes, including *GAPDH*, *UGT1A6*, and c-*jun* were not significantly changed. It is noteworthy that this treatment also reduced ERα mRNA levels to 52%, a level similar to that of cells treated with ERα siRNA (Fig. 6A), suggesting that Fra-2 may play a role in ERα gene expression. Collectively, these results indicate that ERα, c-Jun, and possibly Fra-2 are involved in the up-regulation of *UGT2B15* expression by 17β-estradiol in MCF-7 breast cancer cells.

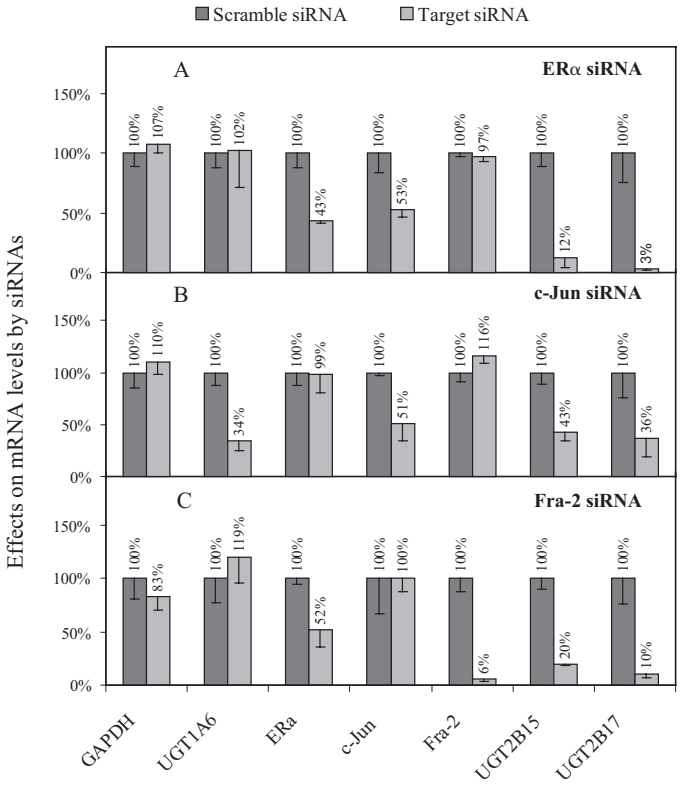

Fig. 6. siRNAs against ERα, c-Jun, and Fra-2 reduce UGT2B15 and UGT2B17 mRNA levels in 17β-estradiol-treated MCF-7 cells. MCF-7 cells were transfected with the indicated siRNAs for 5 h and then cultured in fresh phenol red-free RPMI 1640 medium with 6% DCC-stripped FBS. Forty-eight hours after transfection, cells were treated with 10 nM 17β-estradiol for 24 h and harvested, and target mRNAs were quantified by real-time RT-PCR as described under *Materials and Methods*. After normalizing to 18S rRNA, the relative expression levels of target genes in MCF-7 cells transfected with ERα, c-Jun, or Fra-2 siRNAs were expressed as a percentage of that (set at a value of 100%) in control cells treated with scramble siRNA. Data shown are representative experiments performed in triplicate with error bars representing 1 S.D.

ERα, c-Jun, and Fra-2 Are Recruited to the *UGT2B15* Promoter in MCF-7 Cells after 17β-Estradiol Stimulation. To determine whether ERα, c-Jun, and Fra-2 bind to the endogenous *UGT2B15* promoter, we performed ChIP assays and analyzed specific regions of the UGT2B15 promoter by quantitative real-time PCR with primers as detailed in Table 1. We first demonstrated the efficacy of this method by showing the reported 17β-estradiol-stimulated recruitment of ERα and AP-1 factors, namely c-Jun and Fra-2, to the *pS2/TFF1* promoter, which has an ERE and an AP-1 response element (Fig. 7, A and B) (Baron et al., 2007). At first, we tried to quantify enrichment of a 435-bp region (Table 1, primers 2B15-ChipF3/R1) of the *UGT2B15* promoter, which covered all of the five *cis*-acting elements involved in up-regulation of the *UGT2B15* promoter by 17β-estradiol, as demonstrated by mutagenesis. However, this strategy proved ineffective because of the extremely low efficiency of amplification of the 435-bp fragment by real-time PCR (data not shown).

Because our supershift assays already demonstrated in vitro binding of c-Jun and Fra-2 to the distal AP-1 site (Fig. 4A), we then focused on analysis of a 180-bp region (Table 1, primers 2B15-ChipF2/-R3) of the *UGT2B15* promoter covering only the two AP-1 sites. After MCF-7 cells were treated with 10 nM 17β-estradiol for 2 h, the binding of ERα, c-Jun, and Fra-2 to this region was increased by 8-fold ($p < 0.001$), 2-fold ($p < 0.05$), and 1.7-fold ($p < 0.05$), respectively, compared with controls precipitated by equivalent amounts of the irrelevant preimmune-IgG serum (designated as IgG) (Fig. 7, CD1). This recruitment of ERα, c-Jun, and Fra-2 to the *UGT2B15* promoter was also observed in the analyses of two other promoter regions: a 129-bp region (Table 1, primers 2B15-ChipF1/-R2) covering only the imperfect ERE site (Fig. 7, CD2) and a 247-bp region (Table 1, primers 2B15-ChipF1/-R1) containing all three ERE/half-ERE sites (Fig. 7, CD3). In contrast, there was no statistically significant occupancy ($p > 0.05$ in all cases) of ERα, c-Jun, and Fra-2 on the *UGT2B15* promoter in the vehicle-treated cells for any of the three regions being analyzed (Fig. 7D). We repeated the experiments after 24 h of 17β-estradiol stimulation and found that the binding of ERα, c-Jun, and Fra-2 to the *UGT2B15* promoter remained at a statistically significant level (data not shown). Taken together, these results indicate that ERα, c-Jun, and Fra-2 are recruited to the *UGT2B15* promoter in MCF-7 cells upon 17β-estradiol stimulation.

The AP-1 Sites of the *UGT2B15* Promoter Do Not Function as Classic TPA Response Elements. It is well known that a number of genes are induced by 12-*O*-tetra-

decanoylphorbol 13-acetate (TPA; also known as PMA) through AP-1 binding sites in their promoters. Because of their TPA-inducibility, these AP-1 sites are termed TPA reponse elements (TREs) (Lacroix et al., 2004). As the *UGT2B15* promoter contains two potential AP-1 sites and AP-1 factors bound to the distal site, we investigated whether these AP-1 sites acted as classic TREs.

Treating MCF-7 cells with 100 nM PMA slightly increased UGT2B15 mRNA levels by 1.5-fold, suggesting a marginal effect of PMA on UGT2B15 expression (Fig. 8). In contrast, PMA treatment resulted in a dramatic induction of the mRNA levels of our positive control, the *matrix metalloproteinase 1* (*MMP-1*) gene, a well known PMA-inducible gene (Lacroix et al., 2004) (Fig. 8, inset). We were surprised to find that PMA decreased the activation *UGT2B15* expression by 17β-estradiol by nearly 8-fold. It has been reported that a large number of genes, including ERα and estrogen-induced genes, are down-regulated by PMA (Lacroix et al., 2004). Thus, our observed down-regulation of *UGT2B15* might be simply a result of the PMA-mediated decrease in ERα expression. This assumption was confirmed as we observed a reduction of approximately 3-fold in the ERα mRNA levels regardless of the presence of 17β-estradiol (Fig. 8). As a negative control, the expression of the β-actin gene was not significantly altered under the same conditions (Fig. 8). Collectively, our data suggest that the two AP-1 sites in the *UGT2B15* promoter are insufficient to facilitate a classic inductive response to PMA.

The *UGT2B17* Promoter Responds to 17β-Estradiol via a Mechanism Similar to that of the *UGT2B15* Promoter. The proximal promoter region from nucleotides −1 to −1662 of *UGT2B15* is 91% identical to that of *UGT2B17*. Because of this sequence homology, all five *cis*-activating elements that are involved in 17β-estradiol-mediated *UGT2B15* gene expression, are totally conserved in the *UGT2B17* promoter (Fig. 9A). Because we demonstrated already that the endogenous UGT2B17 mRNA levels in MCF-7 cells treated with 10 nM 17β-estradiol were increased by 78-fold over that of the vehicle-treated cells (Fig. 1), it is reasonable to assume that the *UGT2B17* promoter may also be up-regulated by 17β-estradiol in a manner similar to the *UGT2B15* promoter.

To test this hypothesis, we prepared a reporter construct of 2B17-650/+40Luc by cloning the *UGT2B17* promoter region from nucleotides + 42 to −650 into the pGL3-basic vector and tested its capability to drive transcription upon 17β-estradiol stimulation in MCF-7 cells in transient transfections. As shown in Fig. 9B, compared with that of the controls

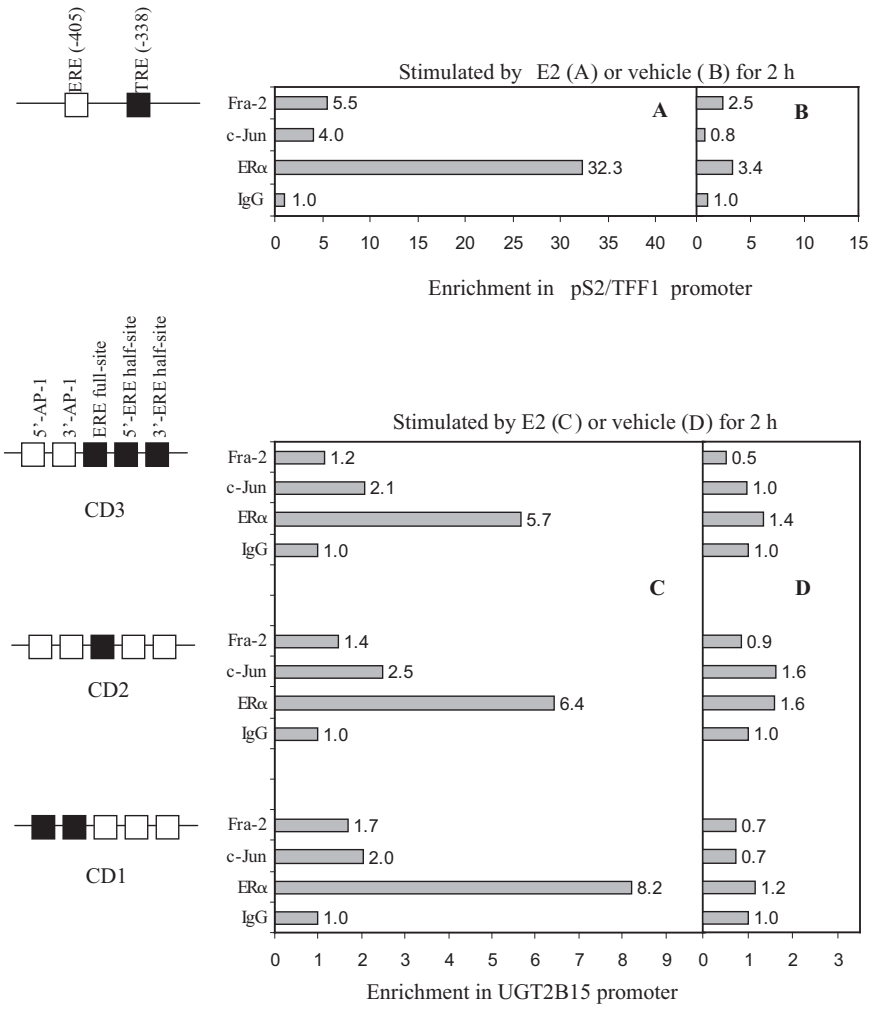

Fig. 7. ERα, c-Jun, and Fra-2 are recruited to the *UGT2B15* proximal promoter in 17β-estradiol-treated MCF-7 cells. Cells precultured in phenol red-free RPMI 1640 medium supplemented with 6% DCC-stripped FBS for 6 days were treated with either 10 nM 17β-estradiol (A and C) or 0.1% ethanol (vehicle) (B and D) for 2 h and subjected to chromatin immunoprecipitation assays, followed by real-time PCR to quantify the precipitated DNA of target sequences as described under *Materials and Methods*. After normalizing to the reference gene, *HCG3*, data were expressed as the -fold enrichment in DNA samples precipitated with 10 μg of each of the antibodies as indicated compared with that (set at a value of 1) in the control DNA samples precipitated from equivalent amounts of preimmune IgG serum (IgG). Data shown are the average of duplicates from one representative experiment. Regions analyzed by PCR in the *pS2/TFF1* promoter (A and B) and the *UGT2B15* promoter (C and D) are indicated with black boxes.

treated with vehicle alone, 17β-estradiol treatment combined with transfected ERα resulted in a nearly 19-fold increase in promoter activity; however, this up-regulation was almost abolished by simply mutating the proximal AP1 site.

We further quantified endogenous UGT2B17 mRNA levels from MCF-7 cells treated with siRNAs directed against ERα, c-Jun, and Fra-2 by quantitative real-time RT-PCR. Our results showed that a significant decrease in the mRNA levels of ERα, c-Jun, and Fra-2 by siRNAs (Fig. 6) respectively reduced UGT2B17 mRNA levels to 3, 36, and 10% of that in cells treated with scramble siRNAs (Fig. 6, A, B, and C). Taken together, these results suggest that the same five *cis*-activating elements confer estrogen-responsiveness to both *UGT2B15* and *UGT2B17* promoters in MCF-7 cells.

Discussion

In this study, we show that expression of both *UGT2B15* and *UGT2B17* is up-regulated by 17β-estradiol in ER-positive breast cancer MCF-7 cells. Furthermore, this effect is mediated by the recruitment of ERα, c-Jun, and Fra-2 to a 282-bp ERU composed of two AP-1 sites, one imperfect ERE site, and two consensus ERE half-sites in the proximal promoters of these *UGT* genes. The induction of *UGT2B15* expression by 17β-estradiol and the contribution of an AP-1 site in this process has been reported previously (Harrington et al., 2006; Kininis et al., 2007). Our work extends these findings by demonstrating the importance of an additional four *cis*-activating elements and the cooperative action of ERα, c-Jun, and Fra-2 in estrogen inducibility of both *UGT* genes.

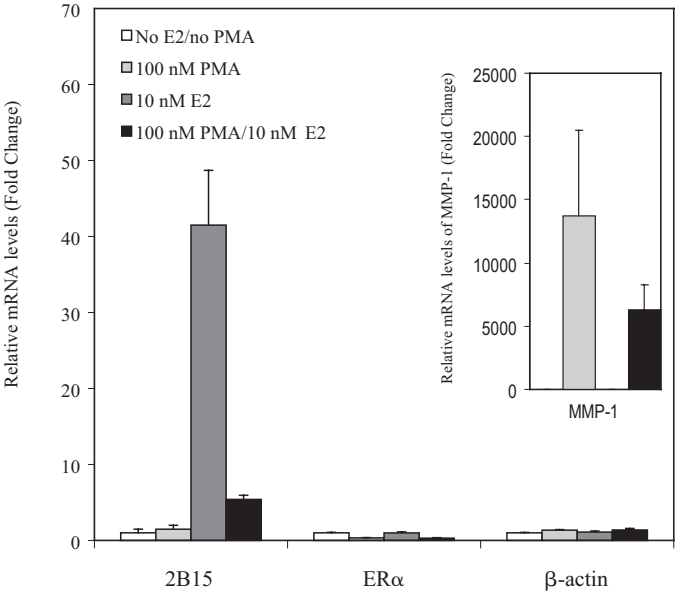

Fig. 8. The phorbol ester PMA does not elevate *UGT2B15* mRNA levels in MCF-7 cells. Cells cultured in phenol red-free RPMI 6140 medium with 6% DCC-stripped FBS for 6 days were treated with 0.1% ethanol (vehicle), 10 nM 17β-estradiol for 24 h, 100 nM PMA for 6 h, or a combination of 10 nM 17β-estradiol for 24 h and 100 nM PMA for 6 h. Cells were harvested and total RNA was extracted, followed by quantification of target mRNAs by real-time RT-PCR as described under *Materials and Methods*. After normalizing to 18S rRNA, the relative mRNA levels of target genes (*UGT2B15*, *MMP-1*, *ERα*, and *β-actin*) were expressed as -fold change over that (set at a value of 1) of the vehicle-treated cells. *MMP-1*, a TPA-inducible gene, acts as a positive control for these experiments. Data shown are a representative experiment performed in triplicate with error bars representing 1 S.D.

Most EREs in other genes are composed of two or more ERE half-sites or imperfect EREs. The ERU of *UGT2B15* and *UGT2B17* has three such sites as determined by mutation analyses. It is noteworthy that these sites in other genes bind ERα poorly in EMSAs (Kraus et al., 1994; Murdoch et al., 1995) but can be identified in ChIP analyses, a phenomenon observed in our study. However, the *UGT2B15* and *UGT2B17* ERU also contains AP sites, because mutation of these sites strongly reduces 17β-estradiol inducibility. Results from our EMSAs showed that AP-1 factors bound the distal AP-1 site mainly as heterodimers c-Jun/Fra-2 (Fig. 4A). These observations were in agreement with our observed 17β-estradiol-induced in vivo recruitment of c-Jun and Fra-2 to the region containing the *UGT2B15* ERU (Fig. 7, C and D). It is noteworthy that our results indicate that the two AP-1 sites do not function as classic TREs. This is in contrast to other genes in which, for example, the binding of c-Jun and Fra-2 to an AP-1 site in the Fra-1 proximal promoter was found to mediate PMA inducibility of this promoter in human lung epithelial A549 cells (Adiseshaiah et al., 2008). A genome-wide screen for in vivo ERα binding sites by ChIP-on-ChIP assays showed that ERα was recruited to the region harboring the *UGT2B15* ERU in MCF-7 cells upon 17β-estradiol-stimulation (Laganière et al., 2005). These findings were verified by our ChIP assays, which clearly demonstrated 17β-estradiol-mediated in vivo recruitment of ERα to the *UGT2B15* ERU (Fig. 7). The significance of ERα, c-Jun, and Fra-2 in the 17β-estradiol-mediated *UGT2B15* induction was further established by our siRNA silencing experiments (Fig. 6).

Taken together, these data indicate that probably both classic (ERα/ERE) and nonclassic (ERα/AP-1) genomic pathways are involved in 17β-estradiol-stimulated *UGT2B15* expression in MCF-7 cells. Given the proximity of the AP-1 and imperfect ERE and ERE-half sites, we propose that transcriptional coactivator complexes associate with these sites after 17β-estradiol treatment and interact to form a super complex that is now permissive for transcriptional activation. A similar mechanism has been proposed to explain the 17β-estradiol-mediated transcriptional synergism between an AP-1 site and an ERE site (separated by 52 bp) on the *pS2* promoter in HepG2 cells (Barkhem et al., 2002) or the insulin-like growth factor-1-induced transcriptional activation of the same *pS2* promoter in MCF-7 cells (Baron et al., 2007). Very recently, studies have shown that 17β-estradiol-modulated *GREB1* gene transcription in MCF-7 cells is mediated by coordinated ERα binding to three consensus EREs, which are located at −21.2, −9.5, and −1.6 kilobases upstream of the closest *GREB1a* transcription start site (Deschênes et al., 2007). The authors detected the formation of 17β-estradiol-induced chromatin loops between each ERE and the transcription start site by chromatin capture assays. Hence, they proposed that these EREs can physically associate with each other through multiple chromatin loops, either in a super complex with the transcription start site or in a transient binary interaction in response to estrogen (Deschênes et al., 2007). In this sense, we cannot rule out the possibility that additional functional imperfect EREs/half-EREs exist in the *UGT2B15* promoter upstream of the ERU identified in the present study, because our bioinformatic analyses revealed the presence of nearly 30 consensus ERE half-sites in that portion of the promoter (data not shown).

Because all five *cis*-activating elements within the *UGT2B15* ERU are completely conserved in the *UGT2B17* promoter at similar positions relative to the translation start site (Fig. 9A), we propose that these same elements most likely account for our observed 17β-estradiol-activated *UGT2B17* gene transcription in MCF-7 cells (Fig. 1). This assumption was supported by the reported 17β-estradiol-induced ERα recruitment to the promoter region containing the *UGT2B17* ERU (Laganière et al., 2005). To further support our hypothesis, we demonstrated by siRNA silencing that 17β-estradiol-stimulated *UGT2B17* gene expression was significantly reduced after repression of ERα, c-jun, and Fra-2 expression by their respective siRNAs (Fig. 6). Furthermore, mutation of the proximal AP-1 site alone almost completely abolished promoter activity (Fig. 9B). However, the functionalities of the remaining four *cis*-activating elements remain to be verified by mutagenesis.

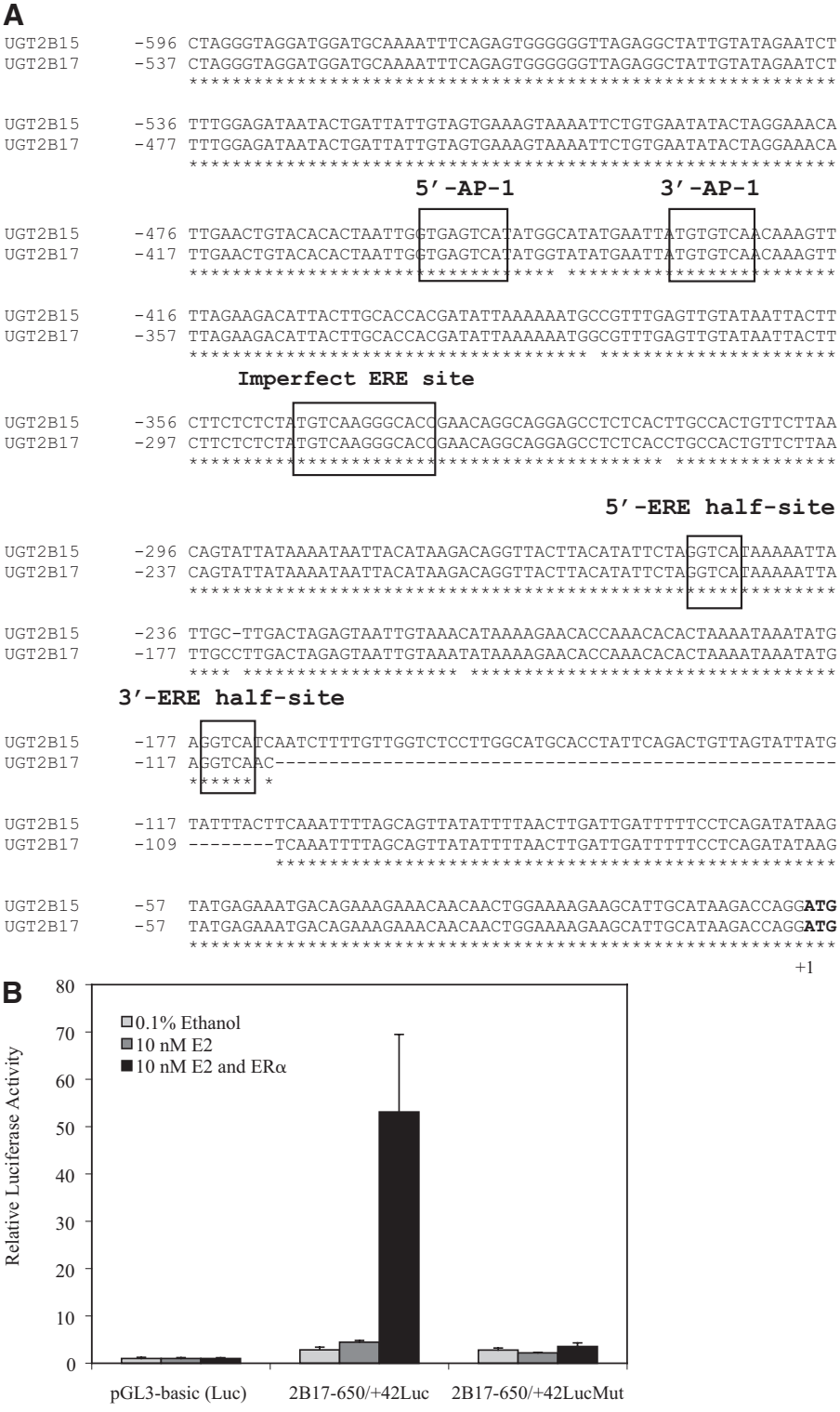

Fig. 9. The *UGT2B17* proximal promoter contains an ERU and is up-regulated by 17β-estradiol in MCF-7 cells. A, the proximal promoters of the *UGT2B15* (top) and *UGT2B17* (bottom) genes are aligned using GenBank records AF179881 and AF179874, respectively. The sequences of the promoter regions are numbered on the left relative to the adenine base of the initiator codon (bold), which is assigned as +1. An asterisk under the sequences indicates conserved nucleotides, and hyphens represent deletions and insertions. The five putative *cis*-activating elements conferring estrogen-inducibility to the *UGT2B15* proximal promoter are boxed and totally conserved in the *UGT2B17* promoter. B, luciferase constructs of the *UGT2B17* promoter carrying the region from nucleotides +42 to −650 relative to the translation start site were transfected into MCF-7 cells with or without cotransfection of ERα expression plasmid. Five hours after transfection, cells were treated with either 10 nM 17β-estradiol or 0.1% ethanol (vehicle). Forty hours after treatment, cells were harvested and assayed for firefly luciferase activities as described under *Materials and Methods*.

Estrogens can negatively regulate their own signaling by multiple mechanisms, as discussed elsewhere in detail (Harrington et al., 2006). One mechanism involves the inactivation and elimination of estrogen by glucuronidation. Whereas UGTs 1A1, 1A3, 1A8, and 1A10 are active in forming the 3-glucuronide, only UGTs 2B7 and 2B17 have the capacity to form the 17β-glucuronide from 17β-estradiol. Under basal conditions, the levels of all these UGTs are very low (Fig. 1) and presumably would have little impact on inactivating estrogen. However, the dramatic increase in the levels of UGT2B17 after 17β-estradiol treatment would increase the capacity of the cell to eliminate 17β-estradiol as the 17β-glucuronide and potentially provide a negative feedback loop controlling the magnitude of the response to active estrogen. In this context, the regulation of *UGT2B17* by 17β-estradiol, which has not been reported previously, would be of significant importance in maintaining estrogen homeostasis. An alternate mechanism for controlling estrogen signaling would be to regulate the removal of precursors required for estrogen synthesis.

It has been reported that 75% of estrogen synthesis before menopause and nearly 100% of estrogen synthesis after menopause occurs in peripheral target tissues from precursor steroids of adrenal origin (Labrie, 1991). The breast is capable of in situ synthesis of both 17β-estradiol and dihydrotestosterone from the common precursor, testosterone, by aromatase and 5α-reductase, respectively, especially after menopause (Sasano et al., 2008). One study even demonstrated that in situ synthesis of 17β-estradiol in breast tumors predominated over uptake from plasma after menopause (Yue et al., 1998). Given that UGT2B15 and UGT2B17 are the only UGTs capable of glucuronidating both testosterone and dihydrotestosterone (Turgeon et al., 2001; Bowalgaha et al., 2007), their induction by 17β-estradiol would lead to removal of these estrogen precursors and hence to a subsequent decrease in estrogen synthesis and estrogen signaling. Thus, up-regulation of UGT2B15 and UGT2B17 levels by estrogens might play a crucial role in the local homeostasis of estrogens, androgens and their precursors within the breast, especially after menopause. The breast and MCF-7 cells contain androgen receptors in addition to estrogen receptors. Because androgens acting through the androgen receptor are antagonistic to estrogen signaling, the capacity of UGT2B15 and UGT2B17 to inactivate dihydrotestosterone may also affect estrogen signaling effects by reducing the antagonism of the androgen receptor signaling pathway in MCF-7 cells and the breast.

In addition to their glucuronidation of steroid hormones, UGT2B15 is also active on the metabolites of these hormones. It has been shown to conjugate endogenous catechol estrogens, such as 4-hydroxyestrone and 4-hydroxyestradiol (Turgeon et al., 2001). 4-Hydroxyestrone and 4-hydeoxyestradiol are present in breast tumors (Rogan et al., 2003) and are believed to be involved in carcinogenesis of breast cancer and other human cancers, partly because their quinone metabolites may react with DNA at purine bases to form depurinating adducts generating highly mutagenic apurinic sites (Cavalieri et al., 2006). Thus, their clearance from the breast through 17β-estradiol-enhanced UGT2B15 and UGT2B17 activity could minimize the exposure of breast tissues to these carcinogens.

In summary, this study identifies c-Jun, Fra-2, and ERα as important factors mediating the response of *UGT2B15* to 17β-estradiol in MCF-7 cells. In the presence of 17β-estradiol, these transcription factors are recruited to a 282-bp ERU in the *UGT2B15* proximal promoter to enhance transcription of this *UGT* gene. This study also identifies *UGT2B17* as a novel estrogen-inducible gene in MCF-7 cells, and our preliminary results suggest that it is up-regulated by 17β-estradiol in a manner similar to that of *UGT2B15*. These studies provide an insight into the mechanisms controlling expression of these major androgen-conjugating UGTs in breast cancer cells and suggest a role for UGT2B15 and UGT2B17 in maintenance of the local homeostasis of sex steroids within the breast.

Acknowledgments

We thank Drs. Robyn Meech and Dione Gardner-Stephen for their valuable advice on technical aspects of the work and their helpful dissussions.

References

Adiseshaiah P, Li J, Vaz M, Kalvakolanu DV, and Reddy SP (2008) ERK signaling regulates tumor promoter induced c-Jun recruitment at the Fra-1 promoter. *Biochem Biophys Res Commun* **371:**304–308.

Andò S, De Amicis F, Rago V, Carpino A, Maggiolini M, Panno ML, and Lanzino M (2002) Breast cancer: from estrogen to androgen receptor. *Mol Cell Endocrinol* **193:**121–128.

Barkhem T, Haldosén LA, Gustafsson JA, and Nilsson S (2002) Transcriptional synergism on the pS2 gene promoter between a p160 coactivator and estrogen receptor-alpha depends on the coactivator subtype, the type of estrogen response element, and the promoter context. *Mol Endocrinol* **16:**2571–2581.

Baron S, Escande A, Albérola G, Bystricky K, Balaguer P, and Richard-Foy H (2007) Estrogen receptor alpha and the activating protein-1 complex cooperate during insulin-like growth factor-I-induced transcriptional activation of the pS2/TFF1 gene. *J Biol Chem* **282:**11732–11741.

Bocchinfuso WP and Korach KS (1997) Mammary gland development and tumorigenesis in estrogen receptor knockout mice. *J Mammary Gland Biol Neoplasia* **2:**323–334.

Bowalgaha K, Elliot DJ, Mackenzie PI, Knights KM, and Miners JO (2007) The glucuronidation of Delta4–3-Keto C19- and C21-hydroxysteroids by human liver microsomal and recombinant UDP-glucuronosyltransferases (UGTs): 6alpha- and 21-hydroxyprogesterone are selective substrates for UGT2B7. *Drug Metab Dispos* **35:**363–370.

Cavalieri E, Chakravarti D, Guttenplan J, Hart E, Ingle J, Jankowiak R, Muti P, Rogan E, Russo J, Santen R, et al. (2006) Catechol estrogen quinones as initiators of breast and other human cancers: implications for biomarkers of susceptibility and cancer prevention. *Biochim Biophys Acta* **1766:**63–78.

Chouinard S, Barbier O, and Bélanger A (2007) UDP-glucuronosyltransferase 2B15 (UGT2B15) and UGT2B17 enzymes are major determinants of the androgen response in prostate cancer LNCaP cells. *J Biol Chem* **282:**33466–33474.

Chouinard S, Tessier M, Vernouillet G, Gauthier S, Labrie F, Barbier O, and Bélanger A (2006) Inactivation of the pure antiestrogen fulvestrant and other synthetic estrogen molecules by UDP-glucuronosyltransferase 1A enzymes expressed in breast tissue. *Mol Pharmacol* **69:**908–920.

Congiu M, Mashford ML, Slavin JL, and Desmond PV (2002) UDP glucuronosyltransferase mRNA levels in human liver disease. *Drug Metab Dispos* **30:**129–134.

Deschênes J, Bourdeau V, White JH, and Mader S (2007) Regulation of GREB1 transcription by estrogen receptor alpha through a multipartite enhancer spread over 20 kb of upstream flanking sequences. *J Biol Chem* **282:**17335–17339.

Gardner-Stephen DA, Gregory PA, and Mackenzie PI (2005) Identification and characterization of functional hepatocyte nuclear factor 1-binding sites in UDP-glucuronosyltransferase genes. *Methods Enzymol* **400:**22–46.

Harrington WR, Sengupta S, and Katzenellenbogen BS (2006) Estrogen regulation of the glucuronidation enzyme UGT2B15 in estrogen receptor-positive breast cancer cells. *Endocrinology* **147:**3843–3850.

Hess J, Angel P, and Schorpp-Kistner M (2004) AP-1 subunits: quarrel and harmony among siblings. *J Cell Sci* **117:**5965–5973.

Heurtaux T, Benani A, Moulin D, Muller N, Netter P, and Minn A (2006) Induction of UGT1A6 isoform by inflammatory conditions in rat astrocytes. *Neuropharmacology* **50:**317–328.

Itäaho K, Mackenzie PI, Ikushiro S, Miners JO, and Finel M (2008) The configuration of the 17-hydroxy group variably influences the glucuronidation of beta-estradiol and epiestradiol by human UDP-glucuronosyltransferases. *Drug Metab Dispos* **36:**2307–2315.

Kato S, Tora L, Yamauchi J, Masushige S, Bellard M, and Chambon P (1992) A far upstream estrogen response element of the ovalbumin gene contains several half-palindromic 5′-TGACC-3′ motifs acting synergistically. *Cell* **68:**731–742.

Kininis M, Chen BS, Diehl AG, Isaacs GD, Zhang T, Siepel AC, Clark AG, and Kraus WL (2007) Genomic analyses of transcription factor binding, histone acetylation, and gene expression reveal mechanistically distinct classes of estrogen-regulated promoters. *Mol Cell Biol* **27:**5090–5104.

Klein-Hitpass L, Kaling M, and Ryffel GU (1988) Synergism of closely adjacent

estrogen-responsive elements increases their regulatory potential. *J Mol Biol* **201:**537–544.
Klein-Hitpass L, Schorpp M, Wagner U, and Ryffel GU (1986) An estrogen-responsive element derived from the 5′ flanking region of the *Xenopus* vitellogenin A2 gene functions in transfected human cells. *Cell* **46:**1053–1061.
Klinge CM (2001) Estrogen receptor interaction with estrogen response elements. *Nucleic Acids Res* **29:**2905–2919.
Kraus WL, Montano MM, and Katzenellenbogen BS (1994) Identification of multiple, widely spaced estrogen-responsive regions in the rat progesterone receptor gene. *Mol Endocrinol* **8:**952–969.
Kushner PJ, Agard DA, Greene GL, Scanlan TS, Shiau AK, Uht RM, and Webb P (2000) Estrogen receptor pathways to AP-1. *J Steroid Biochem Mol Biol* **74:**311–317.
Labrie F (1991) Intracrinology. *Mol Cell Endocrinol* **78**:C113–C118.
Lacroix M, Haibe-Kains B, Hennuy B, Laes JF, Lallemand F, Gonze I, Cardoso F, Piccart M, Leclercq G, and Sotiriou C (2004) Gene regulation by phorbol 12-myristate 13-acetate in MCF-7 and MDA-MB-231, two breast cancer cell lines exhibiting highly different phenotypes. *Oncol Rep* **12:**701–707.
Laganière J, Deblois G, Lefebvre C, Bataille AR, Robert F, and Giguère V (2005) From the Cover: Location analysis of estrogen receptor alpha target promoters reveals that FOXA1 defines a domain of the estrogen response. *Proc Natl Acad Sci U S A* **102:**11651–11656.
Lin CY, Vega VB, Thomsen JS, Zhang T, Kong SL, Xie M, Chiu KP, Lipovich L, Barnett DH, Stossi F, et al. (2007) Whole-genome cartography of estrogen receptor alpha binding sites. *PLoS Genet* **3:**e87.
Mackenzie PI, Bock KW, Burchell B, Guillemette C, Ikushiro S, Iyanagi T, Miners JO, Owens IS, and Nebert DW (2005) Nomenclature update for the mammalian UDP glycosyltransferase (UGT) gene superfamily. *Pharmacogenet Genomics* **15:**677–685.
Marino M, Galluzzo P, and Ascenzi P (2006) Estrogen signaling multiple pathways to impact gene transcription. *Curr Genomics* **7:**497–508.
Murdoch FE, Byrne LM, Ariazi EA, Furlow JD, Meier DA, and Gorski J (1995) Estrogen receptor binding to DNA: affinity for nonpalindromic elements from the rat prolactin gene. *Biochemistry* **34:**9144–9150.
Murphy LC and Watson P (2002) Steroid receptors in human breast tumorigenesis and breast cancer progression. *Biomed Pharmacother* **56:**65–77.
Rogan EG, Badawi AF, Devanesan PD, Meza JL, Edney JA, West WW, Higginbotham SM, and Cavalieri EL (2003) Relative imbalances in estrogen metabolism and conjugation in breast tissue of women with carcinoma: potential biomarkers of susceptibility to cancer. *Carcinogenesis* **24:**697–702.
Safe S, Kim K, and Kim K (2008) Non-classical genomic estrogen receptor (ER)/specificity protein and ER/activating protein-1 signaling pathways. *Journal of Molecular Endocrinology* **41:**263–275.
Sasano H, Suzuki T, Miki Y, and Moriya T (2008) Intracrinology of estrogens and androgens in breast carcinoma. *J Steroid Biochem Mol Biol* **108:**181–185.
Strassburg CP, Oldhafer K, Manns MP, and Tukey RH (1997) Differential expression of the UGT1A locus in human liver, biliary, and gastric tissue: identification of UGT1A7 and UGT1A10 transcripts in extrahepatic tissue. *Mol Pharmacol* **52:**212–220.
Tora L, Gaub MP, Mader S, Dierich A, Bellard M, and Chambon P (1988) Cell-specific activity of a GGTCA half-palindromic oestrogen-responsive element in the chicken ovalbumin gene promoter. *EMBO J* **7:**3771–3778.
Turgeon D, Carrier JS, Lévesque E, Hum DW, and Bélanger A (2001) Relative enzymatic activity, protein stability, and tissue distribution of human steroid-metabolizing UGT2B subfamily members. *Endocrinology* **142:**778–787.
Weisz A, Cicatiello L, Persico E, Scalona M, and Bresciani F (1990) Estrogen stimulates transcription of c-jun protooncogene. *Mol Endocrinol* **4:**1041–1050.
Yue W, Wang JP, Hamilton CJ, Demers LM, and Santen RJ (1998) In situ aromatization enhances breast tumor estradiol levels and cellular proliferation. *Cancer Res* **58:**927–932.

Address correspondence to: Professor Peter Mackenzie, Department of Clinical Pharmacology, Flinders Medical Centre, Bedford Park SA 5042, Australia. E-mail: peter.mackenzie@flinders.edu.au